Thin Solid Films xxx (2016) xxx–xxx

Contents lists available at ScienceDirect

Thin Solid Films

journal homepage: www.elsevier.com/locate/tsf

Solution processing of $CuIn(S,Se)_2$ and $Cu(In,Ga)(S,Se)_2$ thin film solar cells using metal chalcogenide precursors

Panagiota Arnou [a,*], Carl S. Cooper [b], Soňa Uličná [a], Ali Abbas [a], Alex Eeles [a], Lewis D. Wright [a], Andrei V. Malkov [b], John M. Walls [a], Jake W. Bowers [a,*]

[a] Centre for Renewable Energy Systems Technology (CREST), Wolfson School of Mechanical, Electrical and Manufacturing Engineering, Loughborough University, Loughborough, Leicestershire, LE11 3TU, UK
[b] Department of Chemistry, Loughborough University, Loughborough, Leicestershire, LE11 3TU, UK

ARTICLE INFO

Article history:
Received 6 May 2016
Received in revised form 7 September 2016
Accepted 4 October 2016
Available online xxxx

Keywords:
Chalcopyrite
CIGS
Gallium content
Thin-film solar cells
Spray-coating
Solution processing

ABSTRACT

In order to realize the true low cost potential of $Cu(In,Ga)(S,Se)_2$ (CIGS) thin film solar cells, high performance needs to be combined with simple and easily controllable atmospheric-based deposition processes. A molecular solution-based approach for CIGS deposition is proposed, using metal chalcogenide precursors dissolved in an amine-thiol solvent combination. CIGS thin films were sprayed with varying Ga content and the sprayed films were incorporated into solar cells. The effect of the Ga content on the material and device properties is investigated. A champion power conversion efficiency of 9.8% (active area) was achieved, which highlights the potential of this methodology.

1. Introduction

Thin film solar cells are a promising low cost alternative to wafer-based cells, due to materials savings. Among other advantages, these types of solar cells are compatible with low cost, atmospheric-based fabrication processes which can result in significant cost reductions. Such processes are also adaptable to roll-to-roll processing, which brings additional cost benefits [1].

One of the most promising thin film technologies is the chalcopyrite semiconductor $CuInSe_2$ and its alloys, commonly referred to as CIGS. CIGS has a broad single-phase composition range and a tuneable bandgap, by alloying $CuInSe_2$ with S or Ga. High performing devices are commonly obtained with a bandgap of around 1.1–1.3 eV, CGI = [Cu]/([Ga] + [In]) of 0.88–0.95 and GGI = [Ga]/([Ga] + [In]) of ~0.3 [2]. Usually, a graded bandgap as a function of depth is desirable, with higher Ga content towards the back of the absorber [3].

Although the highest performing CIGS devices to date are typically obtained by vacuum co-evaporation, high vacuum deposition equipment requires high capital investment [4]. CIGS can be more cost effective when atmospheric solution processes are used instead, while maintaining high performance. Atmospheric-based processes combine the advantages of high material utilization, low capital investment and a high manufacturing throughput, and as a consequence they are an attractive alternative to vacuum techniques [5]. Pure solution-based approaches in particular offer additional advantages, such as straightforward compositional control simply by modifying the precursor solution [5].

The most promising solution-based approach for CIGS in terms of efficiency, involves the dissolution of metal chalcogenides (Cu_2S and In_2Se_3) and Ga metal in hydrazine [6]. Whilst these precursors are not easily dissolved in common solvents due to their strong covalent bonds, they can be effectively dissolved in hydrazine, in the presence of excess chalcogen [6]. However, the toxic and explosive nature of the solvent makes it difficult to scale up and commercially use this process. This fact has stimulated research on hydrazine-free approaches. For example, recently proposed molecular-based approaches use a combination of dimethyl sulfoxide, thiourea and chlorides [7], butyldithiocarbamic acid [8] or thioacetic acid [9] combined with metal oxides/hydroxides/acetylacetonates. Despite the success of these methods, metal salts and/or oxides are used, which contain impurities that can deteriorate device performance. An alternative molecular-based approach should ideally be developed to involve metal chalcogenides instead, in a similar manner as the hydrazine-based route, but by completely eliminating hydrazine from the process.

An alternative solvent combination of an alkanethiol and 1,2-ethylenediamine has recently been discovered by Brutchey et al. to

* Corresponding authors.
E-mail addresses: P.Arnou@lboro.ac.uk (P. Arnou), J.W.Bowers@lboro.ac.uk (J.W. Bowers).

http://dx.doi.org/10.1016/j.tsf.2016.10.011

dissolve a range of metals, metal oxides, and metal chalcogenides [10, 11]. This solvent mixture has also been used for $CuIn(S, Se)_2$ thin film deposition by dissolving Cu_2S, Cu_2Se, In_2S_3 and In_2Se_3 [12]. However, no working devices were reported due to the high porosity of the spin coated films [12]. Other work suggests that the molecular species in the as-deposited and dried film are partly re-dissolved during the subsequent spinning step, which results in poor material quality [13]. Substitution of spin coating with spraying of the same metal chalcogenide precursor solutions used in our previous work [12], resulted in more densely packed $CuIn(S, Se)_2$ absorber layers and power conversion efficiencies (PCE) up to 8% [14]. The alkanethiol—diamine solvent system was later used for fabrication of $Cu_2ZnSn(S,Se)_4$ solar cells with PCEs exceeding 7%, starting from metal oxides [15]. Pure Cu, In and Ga metals have also been dissolved in the same solvent mixture by heating the solutions for several hours, resulting in CIGS solar cells with PCEs of up to 9.5% [16]. In this work we further explore the potential of this solvent system for CIGS deposition, starting from metal sulphide solution precursors. The Ga content was also varied, in an effort to investigate the effect on the material and device properties.

A repeatable and easily controlled methodology is proposed that allows fine adjustment of the absorber composition. A champion PCE of 9.8% is obtained for a graded bandgap of GGI 0.2–0.3. These results highlight the potential of this approach and it is anticipated that further process optimization will result in higher performance.

2. Experimental details

2.1. Preparation of CIGS precursor solutions

The solutions were prepared targeting a Cu-poor film stoichiometry with varying Ga content. Each individual component solution (i.e., In_2S_3, Cu_2S, Ga) was prepared by dissolution in a mixture of 1,2-ethylenediamine and 1,2-ethanedithiol (vol/vol = 10:1) with a targeted concentration of 0.2 M. The CIGS film composition was controlled by varying the amount of each component solution used. Ga was dissolved in the presence of Se (2 mmol Se per 1 mmol of Ga). It should be noted that no excess chalcogen is required for metal sulphide dissolution, which is the case in the hydrazine-based approach [6]. Hence, elemental Se was only added to the Ga stock solution. The three inks (initially in the form of suspension) were stirred overnight and were converted into optically transparent solutions that are stable for weeks. Cu_2S was converted into a brown solution; Ga stock solution was dark orange and the In_2S_3 solution was colourless. The precursor preparation was performed inside a fume hood, with a nitrogen-purged vial during dissolution. The three component solutions were mixed in certain ratios to form the CIGS precursor solution. The precursor solution was diluted with ethyl acetate (2:1 v/v) and was filtered (0.45 μm polytetrafluoroethylene) prior to the deposition step. After dilution, the precursor solution had a bright orange colour.

2.2. Film preparation and selenization

The spray deposition was performed in ambient atmospheric conditions within a fume hood using a glass chromatography atomizer. The films were sprayed on a molybdenum coated glass substrate placed on a hot plate, controlled at 310 °C. In-between each spray run there was a short drying step for 90 s at the same temperature. After the last deposition/drying cycle, a post-deposition selenization step was performed inside a tube furnace. Unless otherwise stated, there was no intentional bandgap grading in the films and the same solution was used for all the spray runs. In one case, a bandgap grading was attempted by first spraying 3 layers of the solution with GGI = 0.3, followed by two layers of the solution with GGI = 0.2.

For the selenization, two 2.5 × 2.5 cm samples were placed inside a graphite box with Se pellets. The tube was first purged with nitrogen, before setting the starting pressure to 53 kPa. The heating profile lasted for 50 min including ramping (~35 °C/min), which resulted in the complete evaporation of the Se pellets in the box (~300 mg).

2.3. Fabrication of CIGS solar cells

The devices prepared in this work were deposited in the standard stack configuration of ZnO:Al/iZnO/CdS/CIGS/Mo/glass. The CdS layer (~60 nm thickness) was deposited by chemical bath deposition. The intrinsic ZnO and Al doped ZnO layers (~80 nm and 500 nm respectively) were both deposited using RF sputtering. Finally, a top contact grid and MgF_2 anti-reflective (AR) coating were evaporated. Mechanical scribing was performed to isolate each cell of ~0.25 cm^2 area. The grid (0.05 cm^2) shades ~20% of the device area.

2.4. Characterization

Energy Dispersive X-ray spectroscopy (EDS) was used for compositional analysis, with an aperture size of 60 μm and 20 kV operating voltage. A Bruker D2 phaser X-ray diffractometer was used for X-ray diffraction (XRD) analysis, using a Cu-Kα X-ray source and a Lynxeye detector. For the Raman measurements, a Jobin-Yvon LabRam HR system was used to collect un-polarised micro-Raman spectra using a ×50 objective lens and a He-Ne laser (λ = 632.817 nm). The current density/voltage (J-V) characterization of the devices was performed using AM1.5G simulated sunlight from a dual source solar simulator (Wacom, Japan) under 100 mW cm^{-2}, using a calibrated Si reference cell. Prior to the J-V measurements, the cell area was measured using a digital microscope. The external quantum efficiency (EQE) spectra were acquired with chopped light using a Bentham PVE300 system with both Si and Ge reference diodes for calibration. The measurements were performed at 0 V bias with a spectral resolution of 5 nm.

3. Results and discussion

EDS analysis was performed on as-deposited and selenized samples. The chemical composition of the film was determined by averaging the data collected from 2 random points. Table 1 summarizes the composition of each selenized film, as the concentration of each element in relation to (In + Ga) content. The targeted film composition (based on the precursor solution) was $Cu_{0.9}In_{1-x}Ga_xSe_2$, with a constant CGI ratio and GGI varied from 0 to 0.4. It is assumed that S is fully displaced by Se during selenization, as previously observed for sulphide nanocrystal precursors [17]. We have also previously shown for Ga-free samples that S is mostly displaced by Se during the selenization step with comparable selenization conditions [14]. Overall, the atomic ratios of the cations in the films are retained. Previous work on spin coated CIGS films using the alkanethiol—diamine solvent system showed that there was a strong Cu loss during film deposition [13]. This problem is not evident

Table 1
The targeted film composition (based on the precursor solution) and the actual composition of each selenized CIGS sample, estimated with EDS analysis.

		Composition				
Ga/(In + Ga)		Cu	In	Ga	S	Se
0.0	Targeted	0.90	1.00	0.00	0.00	2.00
	Film	0.86	1.00	0.00	0.11	2.19
0.1	Targeted	0.90	0.90	0.10	0.00	2.00
	Film	0.88	0.92	0.08	0.08	2.41
0.2	Targeted	0.90	0.80	0.20	0.00	2.00
	Film	0.93	0.81	0.19	0.72	3.57
0.3	Targeted	0.90	0.70	0.30	0.00	2.00
	Film	0.88	0.72	0.28	0.19	2.04
0.4	Targeted	0.90	0.60	0.40	0.00	2.00
	Film	0.90	0.61	0.39	0.17	2.30

Please cite this article as: P. Arnou, et al., Solution processing of CuIn(S,Se)2 and Cu(In,Ga)(S,Se)2 thin film solar cells using metal chalcogenide precursors, Thin Solid Films (2016), http://dx.doi.org/10.1016/j.tsf.2016.10.011

here, which is most likely related to the different deposition technique used. The formation of fine droplets with spraying may eliminate the re-dissolution of the molecular species during subsequent deposition runs. EDS analysis on as-deposited samples (not shown) shows the anticipated increase of Se incorporation with GGI (Ga is dissolved in the presence of Se), with a composition varying from $Cu_{0.9}InS_2$ to $Cu_{0.9}In_{0.6}Ga_{0.4}$ $S_{1.6}Se_{0.4}$. Finally, it was confirmed that S is mostly displaced by Se during the selenization process. This is justified by the high Se partial pressure favouring the formation of $CuInSe_2$ [17].

The effects of the Ga content on the CIGS thin film properties were investigated with XRD and Raman analysis. The XRD patterns of the films show the same distinct peaks which correspond to the chalcopyrite structure of $CuIn_{0.5}Ga_{0.5}Se_2$ (JCPDS 40-1488). The XRD pattern of the sample with GGI = 0.3 is shown in Fig. 1(a). It was found that the

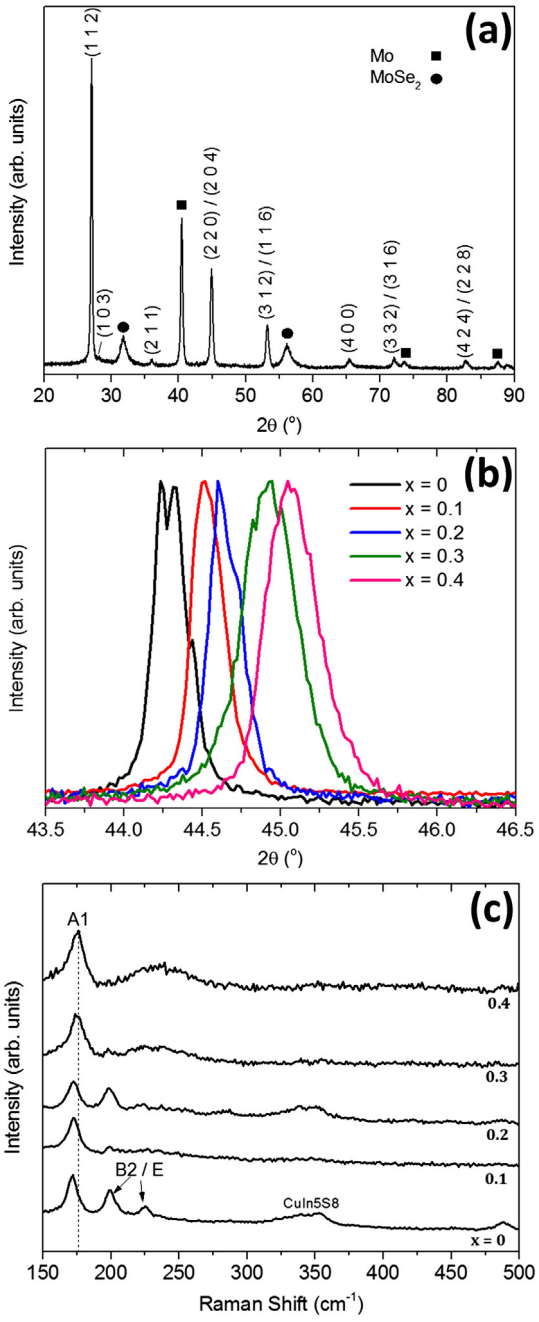

Fig. 1. (a) XRD pattern of a selenized sample with GGI = 0.3. (b) XRD patterns showing the shift in the (220)/(204) diffraction peak with GGI, denoted as x. (c) Raman spectra of the selenized samples with varying GGI.

(112), (220)/(204) and (312)/(116) peaks shift towards higher angles with increasing GGI, which indicates the reduction in the lattice constants, caused by Ga substituting for In [18]. The shift of the (220/204) diffraction peak to higher 2θ values with GGI is shown in Fig. 1(b). Finally, the peak split for GGI = 0 could suggest that there is a phase separation. This peak split is not evident in the other samples, or in previous work for pure $CuInSe_2$ [19]. In the previous work, Cu and In precursors were prepared as a one-pot mixture, which might facilitate the formation of a single phase material.

Fig. 1(c) shows the Raman spectra of selenized films with varying GGI. The most intense Raman peak for $CuInSe_2$ and $CuIn_{1-x}Ga_xSe_2$ films is the A1 zone-centre phonon of the chalcopyrite structure [20]. Overall, the frequency of the A1 mode varies slightly with increasing x (GGI ratio) from 170 cm^{-1} (for x = 0) to 176 cm^{-1} for (x = 0.4). A similar trend has previously been observed for an aqueous spray-pyrolysis approach [18]. The peaks assigned to B2/E vibrational modes of the chalcopyrite are weakened with GGI, with the pure $CuInSe_2$ phase having the strongest peaks. Two additional peaks are evident in the film with GGI = 0 at about 350 cm^{-1} and 490 cm^{-1} and are probably associated to the spinel $CuIn_5S_8$ phase (observed in Cu-poor $CuInS_2$) and to a $Cu_{2-x}S$ phase, respectively. In addition, secondary phases associated with Se-rich composition, such as elemental Se and Cu_xSe are absent in these films [21]. An additional peak is also evident in the Raman spectrum of the film with GGI = 0, at 490 cm^{-1}. This supports the assumption that there is a phase separation for this composition.

The sprayed CIGS films were incorporated into devices. The EQE spectra shown in Fig. 2(a) show a shift in the long-wavelength cut-off to shorter wavelengths. This is indicative of the increased bandgap with Ga content. The drop in EQE at longer wavelengths suggests that the sample is not fully recrystallized throughout its thickness, which is in agreement with our previous work [19]. Fig. 2(b) shows the bandgap values calculated from the EQE data, by plotting $[E \cdot \ln(1\text{-EQE})]^2$ versus E and extrapolating the band edge to the x-axis intercept [19]. The estimated bandgap values are close to the values calculated with the empirical formula for α–$CuIn_{1-x}Ga_xSe_2$: $E_g = 1.65\times + 1.01(1\text{-}x) - 0151(1-x)x$ [22].

The EQE spectrum and the light J-V curve of the highest performing cell are shown in Figs. 2(c) and (d). A champion PCE of 9.8% was obtained for a device with a graded bandgap, with GGI of 0.2 towards the front and 0.3 towards the back of the absorber. The photovoltaic parameters for the best cell on each sample are summarized in Table 2. The anticipated trend of increasing open circuit voltage (V_{OC}) and decreasing short circuit current density (J_{SC}) with GGI ratio is observed. The graded device has a slightly higher J_{SC} compared to the devices with a similar bandgap, which is explained by an improved collection at the long wavelengths. The improved collection could be associated with the back surface field provided by Ga grading, but further analysis is required to support this hypothesis [23].

Based on these results, it is shown that Ga can be conveniently and controllably incorporated in sprayed CIGS films for optimization of the solar cell properties.

4. Conclusions

A molecular solution-based approach is proposed for CIGS deposition, starting from metal chalcogenide precursor solutions. This methodology involves the dissolution of metal sulphides in an amine-thiol combination, which is significantly safer than hydrazine. CIGS thin films were sprayed with varying GGI ratios and were implemented in solar cells. It was shown that the composition and material properties of solution-processed CIGS films can be conveniently controlled using this methodology. A champion PCE of 9.8% was obtained for a device with a targeted graded bandgap. The simplicity of this method and the potential for a fine compositional control make this process highly promising for low cost CIGS fabrication.

Please cite this article as: P. Arnou, et al., Solution processing of CuIn(S,Se)2 and Cu(In,Ga)(S,Se)2 thin film solar cells using metal chalcogenide precursors, Thin Solid Films (2016), http://dx.doi.org/10.1016/j.tsf.2016.10.011

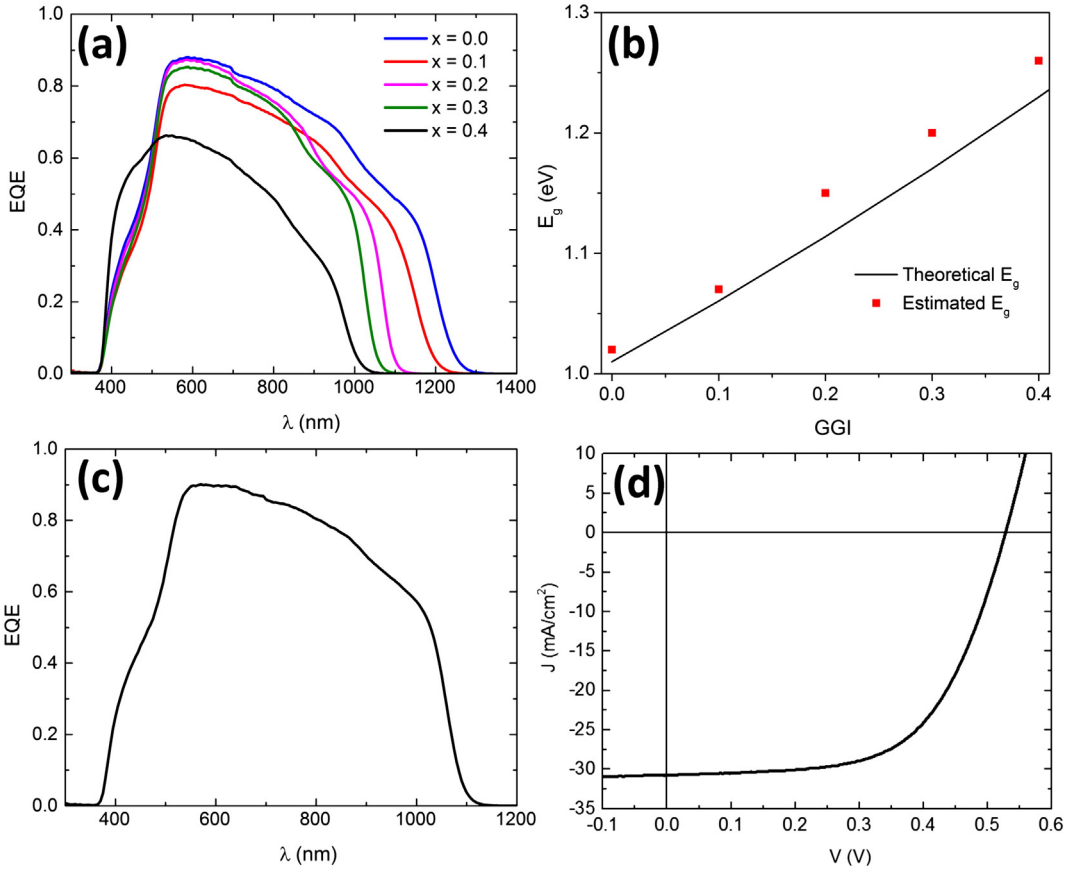

Fig. 2. (a) EQE spectra of CIGS devices with varying GGI. (b) Correlation of the calculated bandgap values (from EQE) with the theoretical values. (c) EQE spectrum and (d) light J-V curve of the best performing device, with GGI = 0.2/03. The PCE, V_{OC}, J_{SC} and fill factor (FF) equal to 9.8% (active area), 528 mV, 30.7 mA cm^{-2} and 60%, respectively.

Table 2
Summary of the J-V characteristics of the best performing cell of each sample with varying GGI.

	Photovoltaic Parameters				
Ga/(In + Ga)	V_{OC} (mV)	Active area J_{SC} (mA/cm^2)	FF (%)	Active area efficiency (%)	Total area efficiency (%)
0.0	466	31.1	49.5	7.18	5.81
0.1	478	29.2	46.5	6.48	5.21
0.2	521	28.4	57.2	8.47	6.83
0.3	416	26.5	51.4	5.68	4.59
0.4	575	19.2	55.2	6.10	4.91
0.2/0.3	528	30.7	60.2	9.76	7.86

Acknowledgements

The authors would like to acknowledge EPSRC Supergen SuperSolar Hub for funding to support this project (EP/N508457/1, EP/J017361/1). The top contact grids and AR coating were deposited at Nanoco Technologies plc (UK). Alex Smith (CREST) assisted with the J-V measurements and Dr. Cary Allen (Nanoco Technologies plc) assisted with the EQE measurements.

References

[1] F. Kessler, D. Herrmann, M. Powalla, Approaches to flexible CIGS thin-film solar cells, Thin Solid Films 480-481 (2005) 491–498.
[2] W.N. Shafarman, L. Stolt, Cu(InGa)Se2 Solar Cells, in: Handb, Photovolt. Sci. Eng, John Wiley & Sons, Ltd, 2005 567–616.
[3] M. Kemell, M. Ritala, M. Leskelä, Thin film deposition methods for CuInSe 2 solar cells, Crit. Rev. Solid State Mater. Sci. 30 (2005) 1–31.
[4] P. Jackson, D. Hariskos, R. Wuerz, O. Kiowski, A. Bauer, T.M. Friedlmeier, M. Powalla, Properties of Cu(In,Ga)Se2 solar cells with new record efficiencies up to 21.7%, Phys. Status Solidi (RRL) 9 (2014) 28–31.
[5] T. Todorov, D.B. Mitzi, Direct liquid coating of chalcopyrite light-absorbing layers for photovoltaic devices, Eur. J. Inorg. Chem. 2010 (2010) 17–28.
[6] T.K. Todorov, O. Gunawan, T. Gokmen, D.B. Mitzi, Solution-processed Cu(In,Ga)(S,Se)2 absorber yielding a 15.2% efficient solar cell, Prog. Photovolt. Res. Appl. 21 (2012) 82–87.
[7] A.R. Uhl, J.K. Katahara, H.W. Hillhouse, Molecular-ink route to 13.0% efficient low-bandgap CuIn(S,Se)2 and 14.7% efficient Cu(In,Ga)(S,Se)2 solar cells, Energy Environ. Sci. 9 (2016) 130–134.
[8] W. Zhao, Y. Cui, D. Pan, Air-stable, low-toxicity precursors for CuIn(SeS) 2 solar cells with 10.1% efficiency, Energy Technol. 1 (2013) 131–134.
[9] Y. Xie, H. Chen, A. Li, X. Zhu, L. Zhang, M. Qin, Y. Wang, Y. Liu, F. Huang, A facile molecular precursor-based Cu(In,Ga)(S,Se) 2 solar cell with 8.6% efficiency, J. Mater. Chem. A 2 (2014) 13237.
[10] D.H. Webber, R.L. Brutchey, Alkahest for V2VI3 chalcogenides: dissolution of nine bulk semiconductors in a diamine-dithiol solvent mixture, J. Am. Chem. Soc. 135 (2013) 15722–15725.
[11] C.L. McCarthy, D.H. Webber, E.C. Schueller, R.L. Brutchey, Solution-phase conversion of bulk metal oxides to metal chalcogenides using a simple thiol–amine solvent mixture, Angew. Chem. Int. Ed. 54 (2015) 8378–8381.
[12] P. Arnou, C.S. Cooper, A.V. Malkov, J.W. Bowers, J.M. Walls, Solution-processed CuIn(S,Se)2 absorber layers for application in thin film solar cells, Thin Solid Films 582 (2015) 31–34.
[13] X. Zhao, M. Lu, M. Koeper, R. Agrawal, Solution-processed sulfur depleted Cu(In,Ga)Se2 solar cells synthesized from a monoamine-dithiol solvent mixture, J. Mater. Chem. A 4 (2016) 7390–7397.
[14] P. Arnou, M.F.A.M. van Hest, C. Cooper, A.V. Malkov, J. Walls, J. Bowers, Hydrazine-Free Solution-Deposited CuIn(S,Se)2 Solar Cells by Spray Deposition of Metal Chalcogenides, ACS Appl. Mater. Interfaces 8 (2016) 11893–11897.
[15] Q. Tian, Y. Cui, G. Wang, D. Pan, A robust and low-cost strategy to prepare Cu 2 ZnSnS 4 precursor solution and its application in Cu 2 ZnSn(S,Se) 4 solar cells, RSC Adv. 5 (2015) 4184–4190.
[16] D. Zhao, Q. Tian, Z. Zhou, G. Wang, Y. Meng, D. Kou, W. Zhou, D. Pan, S. Wu, Solution-deposited pure selenide CIGSe solar cells from elemental Cu, In, Ga, and Se, J. Mater. Chem. A Mater. Energy Sustain. 3 (2015) 19263–19267.
[17] Q. Guo, G.M. Ford, H.W. Hillhouse, R. Agrawal, Sulfide nanocrystal inks for dense Cu(In1 − xGax)(S1 − ySey)2 absorber films and their photovoltaic performance, Nano Lett. 9 (2009) 3060–3065.
[18] M.A. Hossain, Z. Tianliang, L.K. Keat, L. Xianglin, R.R. Prabhakar, S.K. Batabyal, S.G. Mhaisalkar, L.H. Wong, Synthesis of Cu(In,Ga)(S,Se)2 thin films using an aqueous spray-pyrolysis approach, and their solar cell efficiency of 10.5%, J. Mater. Chem. A 3 (2015) 4147–4154.

Please cite this article as: P. Arnou, et al., Solution processing of CuIn(S,Se)2 and Cu(In,Ga)(S,Se)2 thin film solar cells using metal chalcogenide precursors, Thin Solid Films (2016), http://dx.doi.org/10.1016/j.tsf.2016.10.011

[19] P. Arnou, C.S. Cooper, A.V. Malkov, J.M. Walls, J.W. Bowers, Solution-deposited CuIn(S,Se)2 absorber layers from metal chalcogenides, 42nd IEEE Photovolt, Spec. Conf, New Orleans, USA 2015, pp. 1–6.
[20] R. Scheer, A. Pérez-Rodríguez, W.K. Metzger, Advanced diagnostic and control methods of processes and layers in CIGS solar cells and modules, Prog. Photovolt. Res. Appl. 18 (2010) 467–480.
[21] V. Izquierdo-Roca, X. Fontané, J. Álvarez-García, L. Calvo-Barrio, A. Pérez-Rodríguez, J.R. Morante, J.S. Jaime-Ferrer, E. Saucedo, P. Grand, V. Bermúdez, Electrodeposition based synthesis of S-rich CuIn(S,Se)2 layers for photovoltaic applications: Raman scattering analysis of electrodeposited CuInSe2 precursors, Thin Solid Films 517 (2009) 2163–2166.
[22] B.J. Stanbery, Copper indium selenides and related materials for photovoltaic devices, Crit. Rev. Solid State Mater. Sci. 27 (2002) 73–117.
[23] T. Dullweber, G. anna, U. Rau, H. Schock, A new approach to high-efficiency solar cells by band gap grading in Cu(In,Ga)Se2 chalcopyrite semiconductors, Sol. Energy Mater. Sol. Cells 67 (2001) 145–150.

Please cite this article as: P. Arnou, et al., Solution processing of CuIn(S,Se)2 and Cu(In,Ga)(S,Se)2 thin film solar cells using metal chalcogenide precursors, Thin Solid Films (2016), http://dx.doi.org/10.1016/j.tsf.2016.10.011